Rationalizing the Role of Electron/Charge Transfer in the Intramolecular Chemiexcitation of Dioxetanone-Based Chemi-/Bioluminescent Systems

Luís Pinto da Silva[a,b,*] and Joaquim C.G. Esteves da Silva[a,b]

[a] *Chemistry Research Unit (CIQUP), Faculty of Sciences of University of Porto (FCUP), Rua do Campo Alegre 687, 4169-007 Porto, Portugal.*

[b] *LACOMEPHI, GreenUPorto, Department of Geosciences, Environment and Territorial Planning, Faculty of Sciences of University of Porto (FCUP), Rua do Campo Alegre 687, 4169-007 Porto, Portugal.*

** luis.silva@fc.up.pt*

Abstract

The thermolysis of dioxetanones is a key process in the intramolecular chemiexcitation step of several chemi- and bioluminescent reactions. This step is generally explained with mechanisms based on either electron transfer (ET), such as the Chemically Initiated Electron-Exchange Luminescence (CIEEL) mechanism, or charge transfer (CT), such as the Charge Transfer-Initiated Luminescence (CTIL) mechanism. Here, we have used a TD-DFT approach to characterize the thermolysis and chemiexcitation steps of model dioxetanones, to rationalize the role of ET/CT in those intramolecular processes. Our results showed that ET/CT can reduce the activation barrier of the thermolysis reaction, by reducing the repulsion between the reacting fragments (ketone and CO_2 moieties) that originate during peroxide bond breaking. However, in terms of singlet chemiexcitation profiles, those of non-CIEEL/CTIL-based dioxetanones appear to be more efficient than of CIEEL/CTIL-based ones. Furthermore, the ground state to singlet excited state transitions were found to be local excitations, without CT between the peroxide ring and the electron-rich moiety. So, ET/CT appear to be responsible for tuning the activation barrier of the thermolysis reaction, without playing a role in efficient singlet chemiexcitation itself.

Keywords: Bioluminescence; Chemiluminescence; Dioxetanone; CTIL; CIEEL; Density Functional Theory.

1. INTRODUCTION

Chemi- (CL) and bioluminescence (BL) are phenomena in which thermal energy is converted into excitation energy during a chemical/biochemical (respectively) reaction, leading to the emission of visible light [1,3]. One of the remarkable features of both CL and BL is the diminished probability of autofluorescence arising from background signal, as they do not require photo-excitation [4,5]. Given this, these systems have been increasingly used in different areas, such as in real-time imaging [6,7], sensing [8] and even in self-activating sensitizers in cancer therapy [9-11].

Light-emission from CL and BL results from a two-step process [12-14]. First, there is the oxidation of the CL/BL reactant, which leads to the formation of an energy-rich peroxide intermediate. This latter compound is quite unstable and undergoes thermolysis almost instantly (Scheme 1). This decomposition reaction allows for the thermally-activated singlet ground state (S_0) to produce an oxidized chemiluminophore directly in the first singlet excited state (S_1), resulting in singlet chemiexcitation (Scheme 1). One can separate the concepts of thermolysis and chemiexcitation transition, in which S_0 thermolysis is the rupture reaction of the peroxide, and chemiexcitation itself being the process of $S_0 \rightarrow S_1$ excitation at different reaction coordinates. One of the most important types of the energy-rich peroxide intermediates is that of dioxetanone (Scheme 1) [15-20]. This cyclic peroxide is widespread, being responsible for the chemiexcitation of different BL (as in fireflies, imidazopyrazinones and earthworms) and CL (as acridinium esters and 2-coumarones) systems.

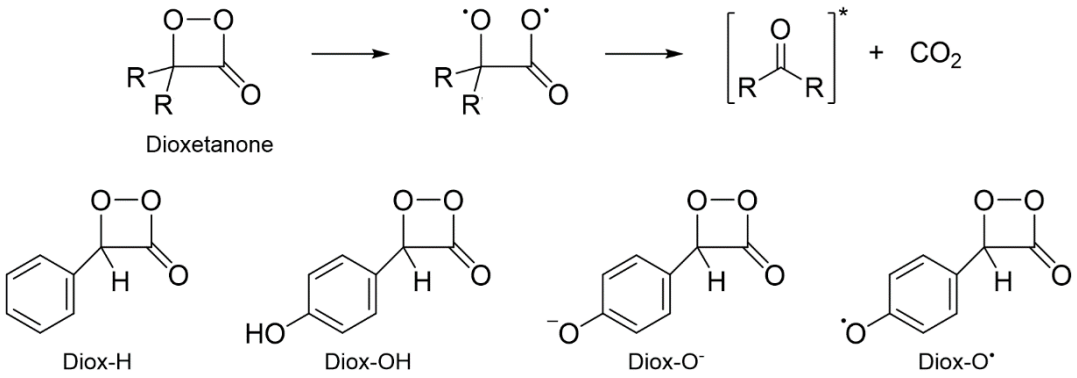

Scheme 1 – Schematic depiction of the chemiexcitation of typical dioxetanones (top). Molecular structures of the studied model dioxetanones (bottom).

One of the main unresolved topics in the study of CL/BL systems is the determination of the mechanism that controls intramolecular singlet chemiexcitation. Namely, despite decades of research, it is still not clear what is the mechanism that allows for singlet chemiexcitation. More

importantly, it is still not understood what allows for an efficient singlet chemiexcitation transition, an essential feature for many practical applications. Thus, it is quite difficult to develop in a rational and target-oriented manner CL/BL systems with innovative and enhanced properties, to be used in novel and/or existent applications with optimized performance.

More specifically, efficient singlet chemiexcitation was first rationalized with the Chemically Induced Electron-Exchange Luminescence (CIEEL) mechanism [21]. CIEEL was thought to occur by electron transfer (ET) from an ionizable electron-rich group to the peroxide with formation of a radical ion pair. Subsequent back ET (BET) would result in efficient singlet chemiexcitation due to charge annihilation. CIEEL was supported by experimental findings that model CIEEL systems could indeed result in efficient chemiexcitation. However, re-evaluations of these model systems by other authors showed significantly lower quantum yields than the ones used to develop and justify the CIEEL mechanism [22,23]. Thus, the basis for CIEEL was proven incorrect, which prompted some researchers to find alternative explanations.

One such alternative is the Charge Transfer-Initiated Luminescence (CTIL) mechanism, in which efficient singlet chemiexcitation results from a more gradual charge transfer (CT) and back CT (BCT), between the ionizable electron-rich group and the peroxide moiety [24,25]. However, CTIL is also unable to account for different results related with CL/BL reactions of dioxetanones. Namely, some neutral dioxetanones (which thermolysis occurred without ET/CT) showed more efficient chemiexcitation profiles than anionic dioxetanones (which thermolysis occurred with ET and/or CT) [26-30]. Furthermore, analysis of different systems indicated that there is no clear relationship between ET-BET/CT-BCT and efficient singlet chemiexcitation, as some dioxetanones with less efficient chemiexcitation underwent thermolysis with relevant ET-BET/CT-BCT, while dioxetanones with more efficient chemiexcitation underwent decomposition with either relevant or negligible ET-BET/CT-BCT between the ionizable electron-rich moiety and the peroxide [24-26,29-32].

Despite both CIEEL and CTIL mechanisms being unable to account for different experimental and theoretical findings, they are still used by different authors to rationalize the chemiexcitation of dioxetanone-based systems [3,12,18,24,25,33-35]. One of the reasons for this is that the S_0 activation energy (ΔE_{act}) for the thermolysis reaction of CIEEL/CTIL-based dioxetanones tends to be significantly lower than for non-CIEEL/CTIL-based dioxetanones (~10 *versus* ~20 kcal/mol) [18,24-35], which should be beneficial for CL/BL reactions. Furthermore, CIEEL/CTIL-based dioxetanones still lead to singlet chemiexcitation, despite theoretical calculations indicating that non-CIEEL/CTIL-based ones possess more efficient chemiexcitation profiles [18,24-35]. Thus, there is the need for rationalizing the role of ET and CT in the chemiexcitation step of the CL/BL reactions of dioxetanones.

Herein, we have characterized the intramolecular chemiexcitation mechanism of a model dioxetanone with different ionization/substitution states/degree (Scheme 1). Our goal here is, by modifying the ionization state of the model dioxetanone, to evaluate the role of both ET and CT between an ionizable electron-rich group and the dioxetanone moiety of the studied compound. With

the obtained information, we expect to clarify the role of ET and CT in the singlet intramolecular chemiexcitation of dioxetanones, which is essential to assess the validity of both CIEEL and CTIL mechanisms. To achieve our goal, we employed a reliable time-dependent (TD) density functional theory (DFT) approach, which was already validated in previous studies of this topic [9,11,20,26,29-32]. The TD-DFT approach was used to calculate the chemiexcitation reaction of a model dioxetanone in different ionization/substitution states/degree (Scheme 1). Namely, the model dioxetanone is composed of the four-membered peroxide ring that is connected to an electron-rich moiety (phenyl groups), due to the importance of ionizable electron-rich groups in both CIEEL and CTIL mechanisms. Four derivatives of the dioxetanone model were studied, which correspond to different ionization/substitution states/degree of the electron-rich moiety (Scheme 1): unsubstituted phenyl (Diox-H), phenol (Diox-OH), phenolate (Diox-O^-) and phenoxyl radical (Diox-$O^\bullet$). It should be noted that these dioxetanone derivatives were not synthesized before (due to difficulty in obtaining this kind of cyclic peroxides), which impairs the direct comparison between theoretical data and experimental results. Nevertheless, they can be used as useful models to understand the role of ionization/substitution degree of the electron-rich moiety in their thermolysis.

2. THEORETICAL METHODS

The theoretical methodology here employed is based on the one used in previous studies of our group [9,11,20,26,29-32]. The geometry optimizations of the S_0 states of the four studied dioxetanones (Scheme 1) were performed at the ωB97XD/6-31G(d,p) level of theory [36], with frequency calculations performed at the same level of theory. We used a closed-shell approach (R) for the reactants and products, and an open-shell (U) one for transition states (TSs). A broken-symmetry (BS) technology was used along with the U approach to make an initial guess for a biradical by mixing the HOMO and LUMO. To ensure that the obtained TSs connected with the desired reactants and products, IRC calculations were performed at the ωB97XD/6-31G(d,p) level of theory. The cartesian coordinates for the TSs obtained for each dioxetanone can be found in Tables S1-S4.

The S_0 energies for the IRC-obtained structures were re-evaluated by single-point calculations at the ωB97XD/6-31+G(d,p) level of theory. The S_1 state for each IRC-obtained structure was calculated with a TD-DFT approach, by performing single-point calculations at the TD ωB97XD/6-31+G(d,p) level of theory on top of the S_0 structures.

ωB97XD was the chosen density functional as it provides accurate estimates for π→π* and n→π* local excitations, and CT and Rydberg states [37]. This functional, as well as other long-range-corrected hybrid exchange-correlated ones, has also been used with success in the study of the chemiexcitation of different peroxides [9,11,20,24-26,29-32].

All calculations were performed *in vacuo*, as the goal here is to study the intrinsic CL/BL properties of a model dioxetanone. Thus, we are focusing on the study of its chemiexcitation

profile while unperturbed by solvent. Finally, all TD-DFT/DFT calculations were made with the Gaussian 09 program package [38].

3. RESULTS AND DISCUSSION

3.1. Study of the S_0 Thermolysis Reaction

This study is divided into two sections, one focused on studying the role of ET/CT in the S_0 thermolysis reaction, and another on studying the same but on the singlet chemiexcitation process. The study of the role of ET/CT is facilitated here by studying a model dioxetanone possessing an electron-rich moiety at different ionization states (neutral, anion, and radical) and substitution degrees (substituted and unsubstituted phenyl groups), as seen in Scheme 1. The first step of this work is then the study of the S_0 thermolysis reaction. As Diox-O$^\bullet$ is in a radical state, its thermolysis reaction was computed at the ground doublet state (D_0). It should be noted that, to our knowledge, this is the first work to study the chemiexcitation of radical dioxetanones.

The potential energy curves for the four studied dioxetanones (Scheme 1) are presented in Figure 1 and correspond to the energies of S_0/D_0 and S_1 states as a function of intrinsic reaction coordinates. It should be noted that Diox-H was recently characterized for the first time by our group in another study, and it is included here for comparison purposes [30]. The calculated S_0/D_0 ΔE_{act} for each thermolysis reaction are the following: 24.0 kcal/mol for Diox-H, 24.2 kcal/mol for Diox-OH, 9.4 kcal/mol for Diox-O$^-$, and 23.1 kcal/mol for Diox-O$^\bullet$. The obtained ΔE_{act} values are in line with existent literature, by showing values in the order of ~20 kcal/mol for neutral species and of ~10 kcal/mol for anionic ones [18,24-35]. According to the literature, the decreased ΔE_{act} of Diox-O$^-$ should result from possible ET and/or CT processes due to the ionization of the hydroxyl group [18,24-35]. Interestingly, these results also show that for neutral species, the introduction of a strong electron-donor (hydroxyl group) has no relevant effect on ΔE_{act}. As for the introduction of the radical moiety, its effects are also quite reduced as its only decreased the ΔE_{act} by ~1 kcal/mol, when comparing with the neutral species. Finally, analysis of Figure 1 indicates that while there are relevant differences between ΔE_{act} for the four dioxetanones, all their thermolysis reactions are highly exothermic (typical for this type of molecules) [18,24-35].

The key geometrical parameters for the thermolysis of dioxetanones are the bond lengths of the peroxide (O-O) and C-C bonds of the four-membered ring (Scheme 1) [18,24-35], which can be found in Figure S1. The thermolysis for all studied species proceeds in a stepwise fashion, by sequential breaking of first the peroxide bond, followed then by C-C cleavage. Furthermore, the determination of $<S^2>$ values of ~1.0 (for S_0 dioxetanones) and higher (for D_0 Diox-O$^\bullet$) from the vicinities of the TS up until the rupture of the C-C bond, for all compounds, indicates the involvement of biradical character. Thus, and consistent with the literature [18,24-35], we can conclude that the thermolysis of the four dioxetanones occurs via a stepwise biradical mechanism.

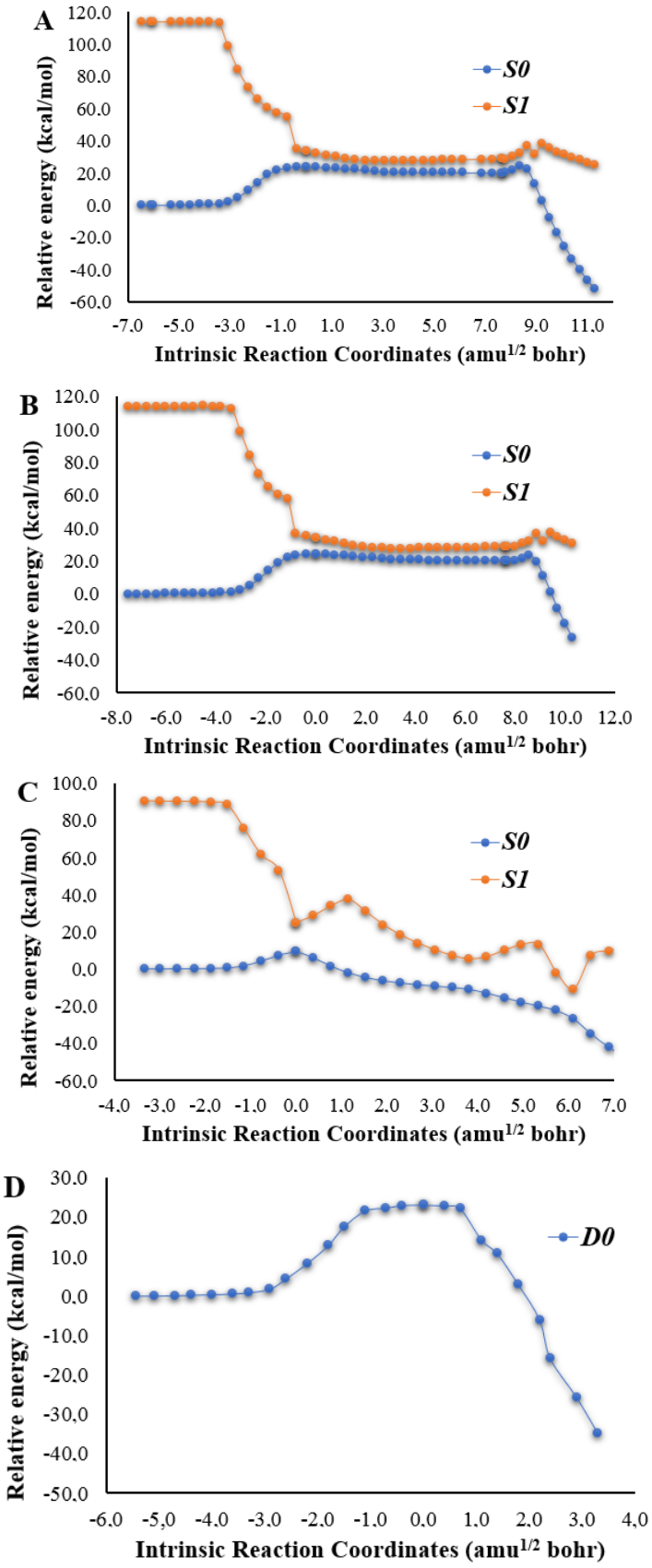

Figure 1 – Potential energy curves of S_0/D_0 and S_1 states as a function of the intrinsic reaction coordinates of Diox-H (A), Diox-OH (B), Diox-O^- (C) and Diox-$O^\bullet$ (D). The curves were calculated at the ωB97XD/6-31+G(d,p) level of theory.

Interestingly, while there is the involvement of a biradical in all reactions, its nature is different for the four dioxetanones. The Mulliken spin density for the TS structure of Diox-H and Diox-OH is located solely on the two oxygen heteroatoms that composed the peroxide bond (Figure 2), which indicates that the biradical is formed due to the homolytic O-O bond breaking, without clear ET features. The Mulliken spin density on the TS of Diox-O$^{\bullet}$ is distributed between the peroxide ring and the electron-rich group (Figure 2). However, analysis of the Mulliken spin density at the reactant structure (Figure S2) reveals that the spin density in the electron-rich group is due to the phenoxyl radical. This means the thermolysis-related biradical also results from homolytic O-O bond breaking, without clear ET character. Finally, for Diox-O^{-} the Mulliken spin density is distributed between the phenolate and the peroxide ring, which indicates the occurrence of ET between the ionized electron-rich group and the dioxetanone moiety. In summary, while neutral and radical dioxetanones undergo thermolysis without clear ET between moieties, the decomposition of Diox-O^{-} proceeds in a manner consistent with the CIEEL mechanism [18,24-35].

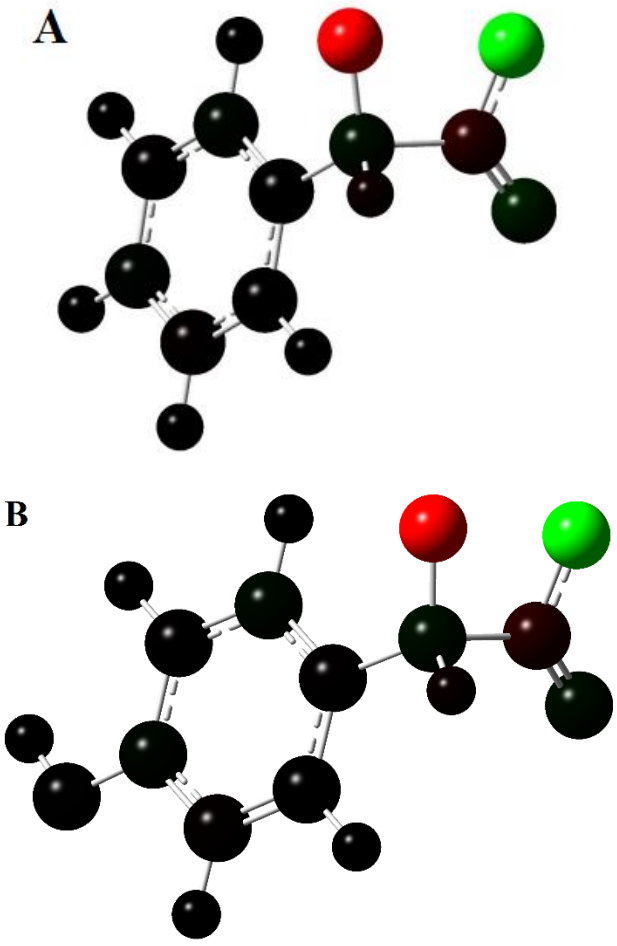

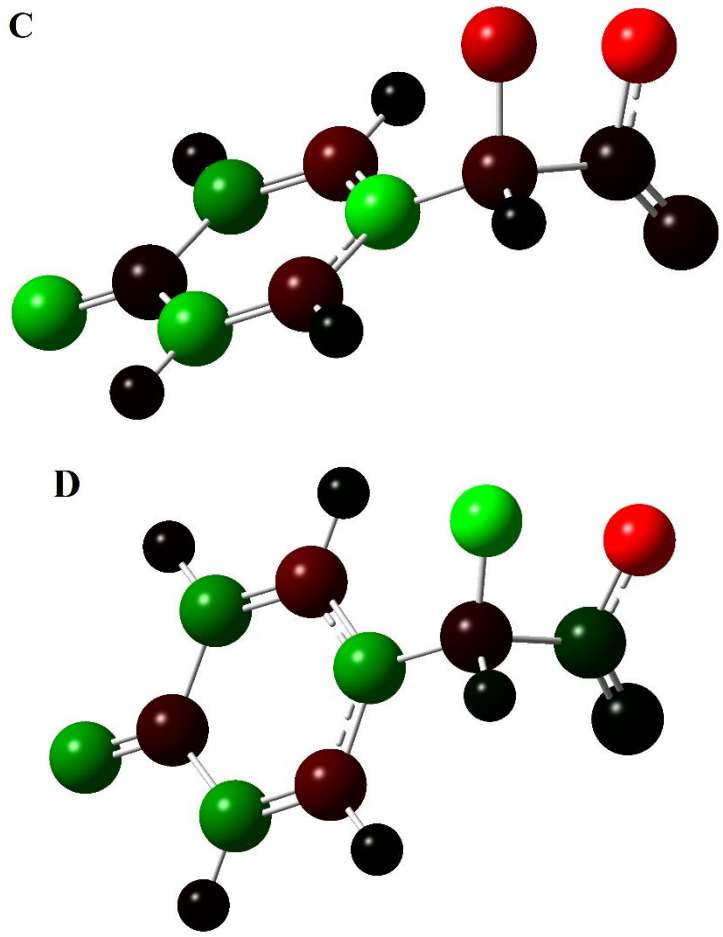

Figure 2 – Mulliken spin density of Diox-H (A), Diox-OH (B), Diox-O^- (C) and Diox-$O^\bullet$ (D) at their TS structures, represented with colour atoms by density.

Given the possible involvement of CIEEL in the thermolysis of the studied model dioxetanone, we proceed to assess the involvement also of the CTIL mechanism. To that end, we measured the NBO charge separation, as a function of intrinsic reaction coordinates, between the phenyl and the cyclic peroxide moieties for all dioxetanones (Figure 3). These results further show that the two neutral species present similar behaviour, while excluding the involvement of the CTIL mechanism from their thermolysis reaction. More specifically, there is no non-negligible CT/BCT between the two moieties for any of the two dioxetanones. There is only relevant CT/BCT (Figure 3) at latter points of the reaction (>8.0 and >8.3 $amu^{1/2}$ bohr for Diox-H and for Diox-OH, respectively), but this occurs after the rupture of the peroxide bond (Figures 1 and S1). Thus, this CT/BCT is not effectively related with the thermolysis reaction. Such profile was already reported for neutral dioxetanones [30]. For the contrary, the thermolysis of Diox-O^- proceeds with obvious CT character (Figure 3). There is the transfer of 0.66*e* from the phenolate group to the dioxetanone ring upon peroxide bond breaking, with subsequent BCT upon the rupture of the cyclic peroxide. The case of Diox-$O^\bullet$ is an interesting one as, like Diox-O^-, its decomposition reaction proceeds with CT character. However, contrary to the case of Diox-O^- in which CT/BCT was more abrupt/immediate, the CT/BCT

observed for Diox-O• is more gradual. The CT is also slightly lower than that of Diox-O$^-$ (0.51*e versus* 0.66*e*). It should be noted that some authors proposed a slightly modified CTIL mechanism, termed gradually reversible CTIL (GR-CTIL), in which CT-BCT is more gradual [24]. Thus, it appears that GR-CTIL is operative for Diox-O•.

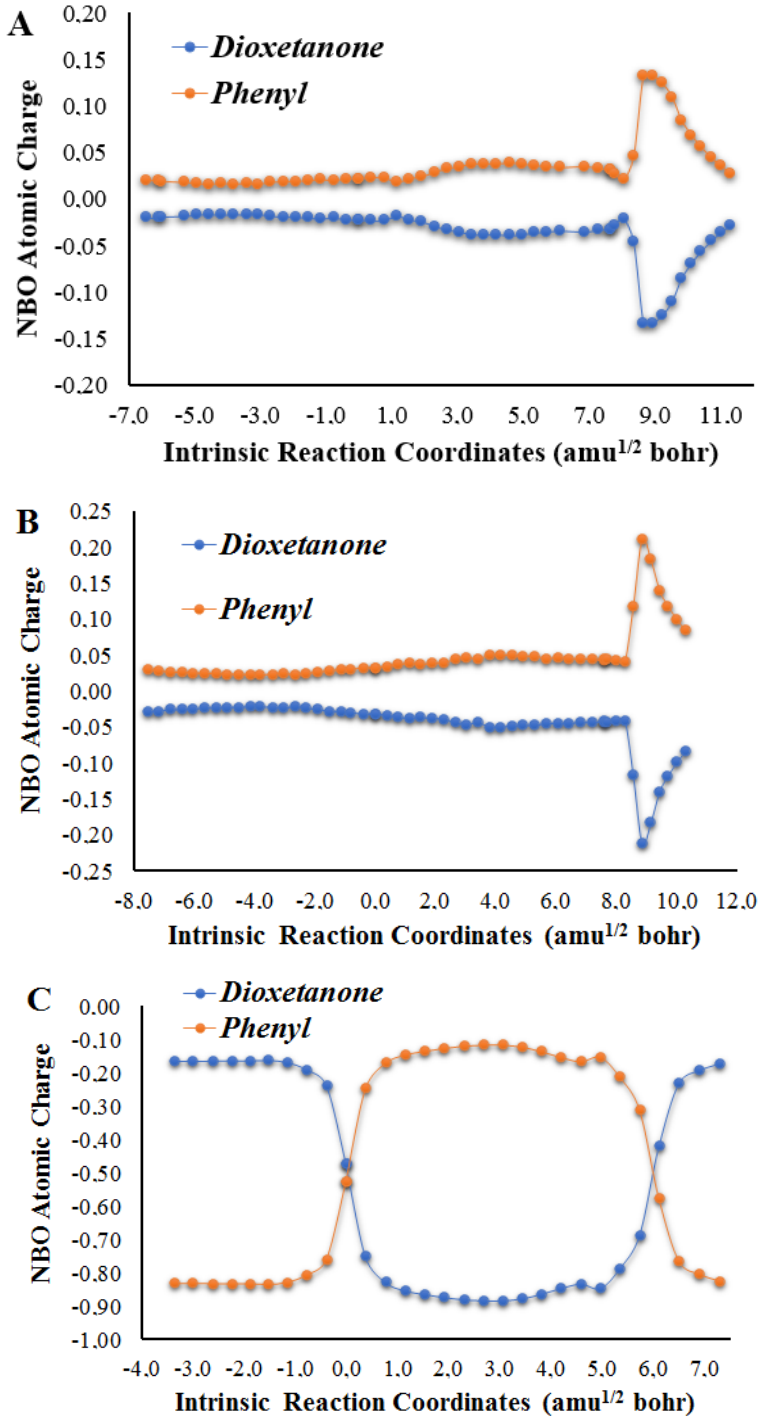

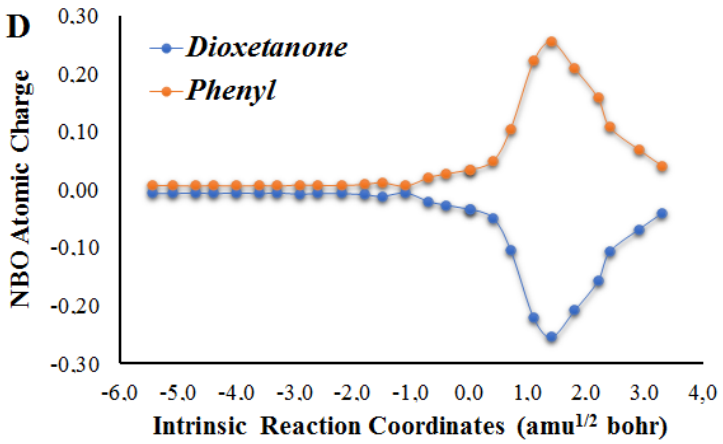

Figure 3 –S_0/D_0 NBO atomic charges as a function of the intrinsic reaction coordinates of Diox-H (A), Diox-OH (B), Diox-O$^-$ (C) and Diox-O$^\bullet$ (D). The charge densities were calculated at the ωB97XD/6-31+G(d,p) level of theory.

So, these results indicate that the thermolysis of Diox-H, Diox-OH and Diox-O$^\bullet$ proceeds without obvious ET character, while deprotonation of the hydroxyl group induces CIEEL-based decomposition. Being of neutral charge also prevents the occurrence of CTIL-based thermolysis for Diox-H and Diox-OH, while ionization of the hydroxyl groups is enough for both Diox-O$^-$ and Diox-O$^\bullet$ to allow for CTIL-based decomposition. However, being an anion or a radical tune the type of CTIL mechanism, with the thermolysis of Diox-O$^-$ proceeding via classical CTIL, while the decomposition of Diox-O$^\bullet$ occurring via GR-CTIL.

In the literature it is described that anionic dioxetanones undergo thermolysis with quite lower ΔE_{act} than their neutral counterparts, as their decomposition occurs via either CIEEL or CTIL [18,24-35]. However, it is still not clearly understood what is the mechanism that effectively allows for the decrease in ΔE_{act} (CIEEL or CTIL, or both?), nor in what way can these mechanisms effectively allow for lower ΔE_{act}. Thus, our next step in this study was for the clarification of this topic.

As consistent with the literature, the ΔE_{act} of Diox-O$^-$ is significantly lower than of the other three dioxetanones. Interestingly, while the thermolysis of Diox-O$^-$ proceeded via both CTIL/CIEEL, the thermolysis of Diox-O$^\bullet$ also proceeded with CTIL but its ΔE_{act} was quite similar to that of the neutral dioxetanones. Therefore, these results indicate that it should be the CIEEL mechanism that allows for the quite lower ΔE_{act} of Diox-O$^-$, when comparing with the other dioxetanones.

To obtain further insight into what controls the ΔE_{act} for the four thermolysis reactions, we used the activation strain model [39,40] to understand the evolution of the potential energy surface ($\Delta E(\zeta)$) between the reactants and the TSs. The activation strain model decomposes the $\Delta E(\zeta)$ into two contributions along the reaction coordinate ζ: $\Delta E(\zeta)_{int}$, which is the interaction energy between the reactants; $\Delta E(\zeta)_{strain}$, which is determined by the structural distortion that the

reactants suffer during the reaction. As these thermolysis reactions are unimolecular processes, this analysis will be made between the resulting fragments of the decomposition reaction: CO_2 and the ketone moiety (Scheme 1). The analysis was made at the reactant and the TS structures for each studied reaction (Table 1). $\Delta\Delta E(\zeta)_{strain}$ is the sum of $\Delta E(\zeta)_{strain}$ for both fragments, with $\Delta E(\zeta)_{strain}$ arising from the difference in strain between the reactant and TS structures for each fragment. $\Delta\Delta E(\zeta)_{int}$ is the difference of $\Delta E(\zeta)_{int}$ between reactant and TS structures for both fragments.

Table 1 – Contributions (in kcal/mol) for $\Delta\Delta E(\zeta)_{int}$ and $\Delta\Delta E(\zeta)_{strain}$ for the $\Delta E(\zeta)$ between the reactant and TS structures of the four studied dioxetanones, calculated by employing the activation strain model [39,40]. Energies were obtained at the ωB97XD/6-31+G(d,p) level of theory.

	$\Delta\Delta E(\zeta)_{int}$	$\Delta\Delta E(\zeta)_{strain}$
Diox-H	33.2	-9.2
Diox-OH	35.0	-10.8
Diox-O^-	22.2	-12.7
Diox-$O^\bullet$	36.1	-13.0

These results show that the ΔE_{act} is determined mainly by $\Delta E(\zeta)_{int}$ for all reactions, as $\Delta\Delta E(\zeta)_{int}$ is positive (indicating reduction of attractive interactions/increase in repulsive interactions during the reaction) and clearly the highest absolute value. $\Delta\Delta E(\zeta)_{strain}$ is smaller for each reaction, with its negative value indicating that this parameter helps to reduce ΔE_{act}. Thus, it appears that the breaking of the peroxide bond leads to relevant repulsive interactions between the two reaction fragments, which are responsible for increasing ΔE_{act}, which is then the energy necessary to overcome these repulsive interactions.

Also of note is that while the $\Delta\Delta E(\zeta)_{int}$ is similar for the neutral species and Diox-$O^\bullet$ (33.2-36.1 kcal mol), this parameter is significantly lower for Diox-O^- (22.2 kcal/mol). Meaning that the lower ΔE_{act} of this latter species results from lower repulsive interactions between fragments. So, given all these results, we can hypothesize that the reason CIEEL is associated with lower ΔE_{act} is that the ET process helps to reduce the repulsive interactions between fragments, which needs to be overcome so that the thermolysis reaction can proceed.

As indicated before, CIEEL consists of ET processes, with a first ET between the electron-rich moiety and the peroxide (which triggers the breaking of the peroxide bond) [21-23]. So, there is the question of how this ET process reduces the ΔE_{act}. One possibility is that the ET process could lead to opposite charges in the fragments of anionic dioxetanones, allowing for attractive electrostatic interactions. However, that is not the case. In Figure S3 is presented the

NBO charge separation between the CO_2 and the ketone moiety of Diox-OH and Diox-O^-, between the reactant and TS, as a function of intrinsic reaction coordinates. While the fragments of Diox-OH are almost neutral in most of the PES region (with slightly increase in opposite charges nearing the TS), both fragments of Diox-O^- are negative with CT approximating the negative charge of both fragments. Thus, ET should not reduce the ΔE_{act} of Diox-O^- by increasing attractive electrostatic interactions.

It should be noted that for dioxetanones in which the peroxide bond breaks homolytically, the σ and σ* orbitals become lone pair orbitals with each oxygen heteroatom retaining one electron of the original O lone pairs (leading to the biradical) [41,42]. Furthermore, it is known that lone pair-lone pair repulsion is a parameter that can affect the energetics of a given system [43-45]. Thus, it is possible that the ΔE_{act} of neutral and radical dioxetanones is higher because the homolytic peroxide bond breaking leads to new lone pairs (in the same plane) in the two oxygen heteroatoms, increasing the lone pair-lone pair repulsion during the thermolysis reaction. As for Diox-O^-, the ET process could lead to delocalization of the electron density between the molecule, reducing the lone pair-lone pair repulsion between the oxygen heteroatoms that constituted the peroxide bond.

To assess the validity of this hypothesis, we plotted the isosurface of the electron spin density of the TS structure of both Diox-OH and Diox-O^- (Figure S4). This was made with the Multiwfn software [46], by using as basis the Gaussian 09 calculations at the ωB97XD/6-31+G(d,p) level of theory. In fact, for Diox-OH (Figure S4), the electron spin density resides mainly on the two oxygen heteroatoms that constituted the peroxide bond, with an isosurface compatible with in-plane lone-pairs. However, this not the case for Diox-O^-. There is indeed electron spin density on the two oxygen heteroatoms, but the size of isosurface is quite smaller than that of Diox-OH (in those atoms). Furthermore, there is also relevant electron spin density at the phenolate oxygen. Thus, this indicates that there is delocalization of the electrons involved in the peroxide bond between the molecule, reducing the electron density at the new in-plane lone pairs of the dioxetanone ring (after peroxide bond breaking). This should reduce the lone pair-lone pair repulsion between them, thereby reducing the repulsive interaction between fragments.

We performed also a NBO analysis for the TS structures of Diox-OH and Diox-O^-. For Diox-OH, NBO analysis revealed both for both α and β spin orbitals the presence of in-plane lone pairs on oxygen heteroatoms, which should result from peroxide bond breaking (Figure S5). The occupancy values for the lone pair on the ketone's oxygen heteroatom were of 0.15 and 0.88 (α and β spin orbitals, respectively), and of 0.94 and 0.17 for the CO_2's oxygen (α and β spin orbitals, respectively). Interestingly, NBO analysis only showed for Diox-O^- the presence of in-plane lone pairs on the oxygen heteroatoms for β spin orbitals, and not for α spin orbitals (Figure S6). The occupancy numbers were of 0.72 for ketone's oxygen and of 0.74 of CO_2's oxygen. These results also indicate that the electron density the lone pairs that result from peroxide bond breaking are

lower for Diox-O^-, as a result from ET between the electron-rich moiety and the dioxetanone ring. This show then favour lowering the repulsion between these lone pairs, and possibly between them and the other oxygen heteroatoms lone pairs already existent at the beginning of the reaction.

Further support for this is the increase in peroxide (O-O) bond length between the reactant and TS structures for the different dioxetanones: 0.62 Å for Diox-H, 0.61 for Diox-OH, 0.26 Å for Diox-O^-, and 0.51 Å for Diox-$O^\bullet$. These higher increases for neutral and radical dioxetanones are in line with the need for accommodating for increased repulsions between the two oxygen heteroatoms.

Nevertheless, further research should be performed on this topic to both confirm the role of lone pair-lone pair repulsion and assess the existence of other contributions of the ET process to decrease the ΔE_{act} of the S_0 thermolysis reaction of dioxetanones.

In summary, our results allow us to hypothesize that CIEEL decreases the S_0 ΔE_{act} of anionic dioxetanones, by favouring a heterolytic cleavage of the peroxide bond and reducing the lone pair-lone pair repulsion of new lone pairs of oxygen heteroatoms. CTIL was not found to have relevant effect on the S_0 thermolysis reaction by itself, with CT/BCT being possibly a consequence of ET-BET (as postulated by CIEEL).

3.2. Study of S_1 Chemiexcitation Transitions

After evaluating the role of ET and CT processes on the thermolysis reaction, we then proceeded to evaluate their role on the S_1 chemiexcitation step. As we are now interested in singlet chemiexcitation, in this section we will just analyse Diox-H, Diox-OH and Diox-O^-. The potential energy curves of the S_1 states (as well as S_0) for the three dioxetanones, as a function of intrinsic reaction coordinates, can be found on Figure 1.

Diox-H and Diox-OH possess the typical chemiexcitation profile of neutral dioxetanones [20,24,26,29-33]. The S_0 PES consists of a large and flat biradical region between the TS and the rupture of the peroxide ring, with lengths of 10.5 and 10.7 $amu^{1/2}$ bohr for Diox-H and Diox-OH, respectively. More importantly, both S_0 and S_1 are nearly-degenerated/degenerated within the large and flat biradical region, with energy gaps of 6.1-9.9 and 6.0-11.5 kcal/mol for for Diox-H and Diox-OH, respectively. This type of profile can be associated with efficient singlet chemiexcitation, as there are near-infinite possibilities for non-adiabatic transitions [20,24,26,29-33,41,42]. Furthermore, multireference calculations are expected to predict even smaller energy gaps, due to an energy error in this region by the TD-DFT approach resulting from spin contamination in the reference state by using BS technology [20,24,26,29-33,41,42]. Nevertheless, TD-DFT calculations have been extensively shown to provide accurate qualitative results for these system [20,24,26,29-33,41,42], providing a less demanding alternative to multireference methods in terms of computational power.

Diox-O^- also shows a chemiexcitation profile similar to what is described in the literature for anionic dioxetanones [20,24,26,29-33]. Namely, the biradical S_0 region is not flat and is quite shorter (6.1 $amu^{1/2}$ bohr) than the ones found for neutral dioxetanones (10.5-10.7 $amu^{1/2}$ bohr). There is also no region of degeneracy, as besides three reaction coordinates, the energy gap is always higher than 17.1 kcal/mol. The energy gaps for these three coordinates are also quite higher than the ones found for neutral dioxetanones (6-0-11.5 kcal/mol): 15.5 kcal/mol at 0.0 $amu^{1/2}$ bohr, 16.4 kcal/mol at 2.3 $amu^{1/2}$ bohr, and 15.9 kcal/mol at 6.1 $amu^{1/2}$ bohr.

Thus, our calculations indicate that dioxetanone derivatives with -OH group attached to electron-rich moieties should lead to more efficient singlet chemiexcitation ($S_0 \rightarrow S_1$ chemiexcitation) than derivatives with deprotonated -O^- groups. This is due to lower energy gaps between S_0 and S_1 states, and for the larger portion of the PES where these states are close enough for transition, associated with neutral dioxetanones [20,26,29-33]. These conclusions are also supported by experimental findings regarding the chemiluminescent reaction of imidazopyrazinones, in which higher light emission was found at lower pH values [26,31]. This pH-dependency was attributed to the ionization state of the involved dioxetanone, in which neutral dioxetanones lead to higher chemiexcitation efficiencies while anionic ones lead to lower chemiexcitation efficiencies [26,29,31]. This finding, that neutral dioxetanones lead to higher efficiencies was also supported by other authors based on their own experimental observations of the CL reactions of imidazopyrazinones [27,28,46] Furthermore, Naumov *et al.* also provided indirect spectroscopic evidence that the BL reaction of *Cypridina* luciferin (an imidazopyrazinone molecule) proceeds via the thermolysis of a neutral dioxetanone [47]. It should be noted that different theoretical calculations agree that the thermolysis of neutral imidazopyrazinone dioxetanones lead to efficient singlet chemiexcitation by presence of a large and flat biradical region in which S_0 and S_1 are degenerated/nearly-degenerated (which is not explained by ET/CT processes) [20,24-26,29-33], as consistent with our present results. Furthermore, while there is still little direct experimental evidence, there are indirect experimental and theoretical results related to the firefly BL system that indicates that the deprotonation of the hydroxyl-benzothiazole group of firefly dioxetanone only occurs in conditions not in line with firefly BL reaction [48]. Also, the experimental monitoring of the excited-state dynamics of the oxyluciferin light-emitter in firefly luciferase revealed contributions to the light emission of species with protonated hydroxyl-benzothiazole groups of between 18.3% and 57.6% (depending on the pH) [49]. These values support the chemiexcitation of firefly oxyluciferin from a protonated firefly dioxetanone species, with light-emission from deprotonated species being potentially attributed to the photoacidic nature of this bioluminophore [50]. Finally, theoretical calculations also verified that the thermolysis and chemiexcitation of firefly dioxetanone occurs without relevant ET/CT, further supporting our results [51].

It should be noted that, besides intramolecular CL/BL reactions, dioxetanones are also capable to induce CL via intermolecular ET/CT-catalysed decomposition reactions involving a fluorescent activator [23,52,53]. These intermolecular charge delocalization-based reactions are known to possess low efficiency, which has been attributed to sterical hindrance in the formation of the supramolecular complex between the peroxide and the activator [23,52,53]. While we do not dispute the role played by steric effects, our results do indicate that these low efficiencies could also be explained by the notion that ET/CT have no clear relationship with efficient singlet chemiexcitation regarding dioxetanones. Nevertheless, some care must be taken before extrapolating our conclusions regarding intramolecular systems with that of intermolecular systems, as their chemiexcitation and light-emission proceeds via distinct pathways. That is, in intramolecular systems occurs the direct chemiexcitation of the carbonyl reaction fragment, which is the light-emitter. By their turn, in intermolecular systems, while information regarding the process is still limited, it is known that it is the activator to be chemiexcited via internal conversion upon ET/CT in the supramolecular conformation [52,53]. Thus, further comparative investigation must be made between intramolecular/intermolecular systems, so we can understand how our results can be extrapolated (or not) to intermolecular systems.

More importantly, as seen before, both neutral species decompose via non-CIEEL/CTIL pathways, while Diox-O^- decomposed via CIEEL/CTIL ones. Thus, these data do indicate that CIEEL and CTIL cannot explain efficient singlet chemiexcitation transitions, as indicated previously [20,24,26,29-33].

At this point, it should be noted that the involvement of CIEEL and CTIL in the chemiexcitation step is generally evaluated in terms of ET/CT during the S_0 thermolysis. However, these mechanisms (especially CTIL) could be also involved in the chemiexcitation step in terms of the $S_0 \rightarrow S_1$ transition. That is, if the associated excitations possesses or not CT character.

To further characterize the chemiexcitation step, we have then evaluated quantitatively the electron excitation at different reaction points in terms of associated hole and electron distribution in the whole space. This was made with the Multiwfn software [54], by using as basis the Gaussian 09 calculations at the ωB97XD/6-31+G(d,p) level of theory. The analysis of the $S_0 \rightarrow S_1$ excitation was made for both Diox-OH and Diox-O^- at three different intrinsic reaction coordinates, for each molecule. For Diox-O^-, we considered the three reaction coordinates with lowest S_0 - S_1 energy gaps: 15.5 kcal/mol at 0.0 $amu^{1/2}$ bohr, 16.4 kcal/mol at 2.3 $amu^{1/2}$ bohr, and 15.9 kcal/mol at 6.1 $amu^{1/2}$ bohr (Figure 1). For Diox-OH, we considered the reaction coordinate with lowest energy gap (6.0 kcal/mol at 2.3 $amu^{1/2}$ bohr), and the first and last coordinates for the region of degeneracy: 10.2 kcal/mol at 0.0 $amu^{1/2}$ bohr, and 8.2 kcal/mol at 8.6 $amu^{1/2}$ bohr (Figure 1).

Table 2 – S_r, *D* (in Å) and *t* indexes determined upon quantitative characterization of hole and electron distribution upon electron excitation, calculated with Multiwfn software [54] based on computations at TD ωB97XD/6-31+G(d,p) level of theory. The obtained parameters are of $S_0 \rightarrow S_1$ transitions at different intrinsic reaction coordinates ($amu^{1/2}$ bohr) of the thermolysis reaction of Diox-O^- and Diox-OH.			
Diox-O^-			
Reaction Coordinates ($amu^{1/2}$ bohr)	S_r index	*D* index (Å)	*t* index
0.0	0.905	0.359	1.245
2.3	0.653	0.316	-0.807
6.1	0.888	0.661	-0.894
Diox-OH			
Reaction Coordinates ($amu^{1/2}$ bohr)	S_r index	*D* index (Å)	*t* index
0.0	0.630	0.247	-0,513
2.3	0.647	0.116	-0,557
8.6	0.724	0.574	-0,714

Multiwfn allows to perform a quantitative characterization of the hole and electron distribution, upon electron excitation, by calculating different parameters [54]. S_r index characterizes the overlapping extent of hole and electron (its theoretical upper limit is 1.0). *D* index (in Å) characterizes the total magnitude of CT length. The *t* index is designed to measure the separation degree of the hole and electron in the CT direction. If this index is negative, it means that the hole and electron are not substantially separated due to CT. Clear separation of hole and electron distributions should lead to positive values for the *t* index. The obtained values for these parameters can be found on Table 2 for both Diox-OH and Diox-O^-. The simultaneous distribution of hole and electron for the different coordinates of Diox-O^- are present on Figure 4, while the same distribution of Diox-OH are found on Figure 5. We also measured with Multiwfn the charge density difference (CDD) between the S_0 and S_1 states for the different reaction coordinates for the studied dioxetanones, with the resulting isosurfaces being found on Figures S7 (Diox-O^-) and S8 (Diox-OH).

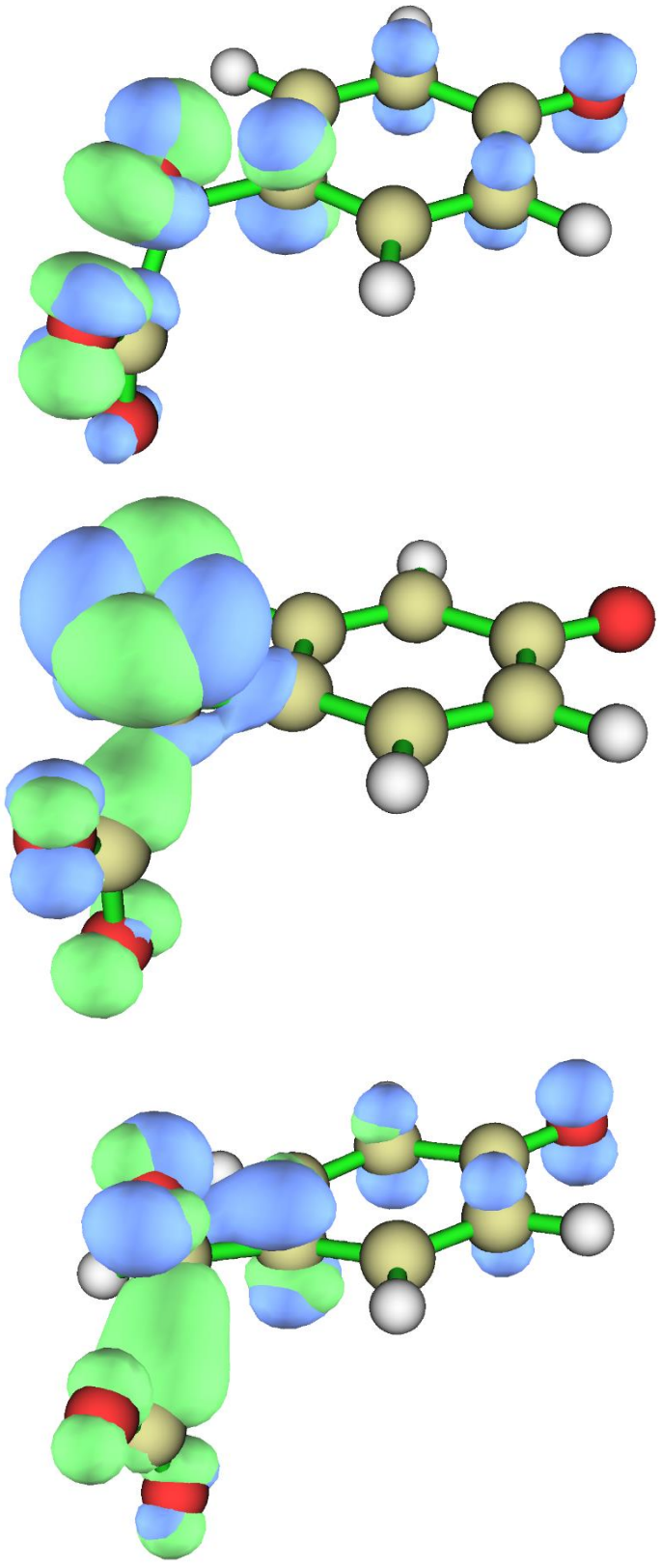

Figure 4 – Simultaneous distribution of hole (in blue) and electron (in green) for $S_0 \rightarrow S_1$ transitions at the following intrinsic reaction coordinates of the thermolysis reaction of Diox-O^-: 0.0 (top), 2.3 (middle) and 6.1 (bottom) $amu^{1/2}$ bohr. The distributions were obtained with Multiwfn [46] based on TD ωB97XD/6-31+G(d,p) calculations.

The *t* index measured for the three coordinates of Diox-O^- is clearly negative, which means that there is no substantial separation between hole and electron due to CT. The values found for the *D* index are quite small (0.316-0.661 Å). Finally, the obtained values for the S_r index (0.653-0.905) clearly indicates than more than the half part of the hole and electron have perfectly matched. These parameters indicate that the studied $S_0 \rightarrow S_1$ transitions for Diox-O^- are of the local excitation (LE) type, and do not correspond to CT excitations. This is also supported by analysis of the simultaneous hole and electron distribution (Figure 4), with green representing the electron distribution and blue the one corresponding to the hole. It can be clearly seen that both the hole and electron are clearly located on the peroxide ring. There are some differences for the coordinate at 6.1 $amu^{1/2}$ bohr, as there is a slight delocalization of both the hole and electron into the phenolate moiety (consistent with the higher *D* index). However, there is still relevant overlap between the hole and electron in that moiety. Finally, the CDD isosurfaces for Diox-O^- are present in Figure S7, with green and blue corresponding to increase and decrease of the excited state density with respect to the ground state density. As consist with the previous results, the changes in charge density between states occur mainly on the peroxide ring, with limited contribution from the ionized electron-rich moiety.

As for Diox-OH, negative *t* index, high S_r index and low *D* index indicates also that the studied $S_0 \rightarrow S_1$ transitions for this species are of the LE type. Analysis of the simultaneous distribution of hole and electron (Figure 5) and the CDD isosurfaces (Figure S8), showed the electron excitation occurs mainly on the peroxide ring with very limited contribution from the phenol moiety.

In summary, we have found that the chemiexcitation profile of dioxetanones that decompose via non-CIEEL/CTIL appears to be more efficient than the ones presented by dioxetanones associated with CIEEL/CTIL pathways. Furthermore, we observed that the chemiexcitation transitions for both types of molecules are of the LE type, not being of CT character. The electron excitation is also located mainly on the peroxide ring, without relevant contribution from the electron-rich moiety. Thus, it can be stated that there is no involvement from CIEEL/CTIL in the chemiexcitation transitions, as there was not found relevant CT/ET between the electron-rich moiety and the peroxide, during electron excitation. Nevertheless, it should be said that while CIEEL/CTIL appear to not be the most efficient mechanism for high chemiexcitation yield, they could still be operative in "real-world" CL and BL reactions. That is, given that these mechanisms still allow for chemiexcitation and that their associated ΔE_{act} is significantly lower than that of non-CIEEL/CTIL pathways, the former could still be more favourable. Despite that, it should be clear that these mechanisms should not be used for justifying higher chemiexcitation yields when in comparison with lower yields, as their benefit appears to be on decreasing the ΔE_{act} of the thermolysis reaction. More specifically, charge delocalization

processes might be involved in efficient CL/BL, but some care must be taken before attributing to these processes an ability to induce efficient $S_0 \rightarrow S_1$ transitions at each reaction coordinate. Instead, charge delocalization processes appear to be relevant at the S_0 level to allow the S_0 reactions to proceed via energetically feasible activation barriers. Thus, further studies should be focused on assessing the energetic feasibility of the S_0 thermolysis reaction of neutral dioxetanone systems with electron-rich moieties.

Finally, it should be mentioned that there is experimental evidence for intramolecular ET in the decomposition of other types of cyclic peroxides, the dioxetanes, with it being more relevant for the chemiexcitation pathway of these peroxides [55-57]. Thus, some relevant differences appear to exist between dioxetanes and dioxetanones, which should not be so unexpected given that despite their similarities, they are different classes of cyclic peroxides. Nevertheless, this mean that in the future, comparative studies should be performed to further understand the similarities and differences between dioxetanes and dioxetanones.

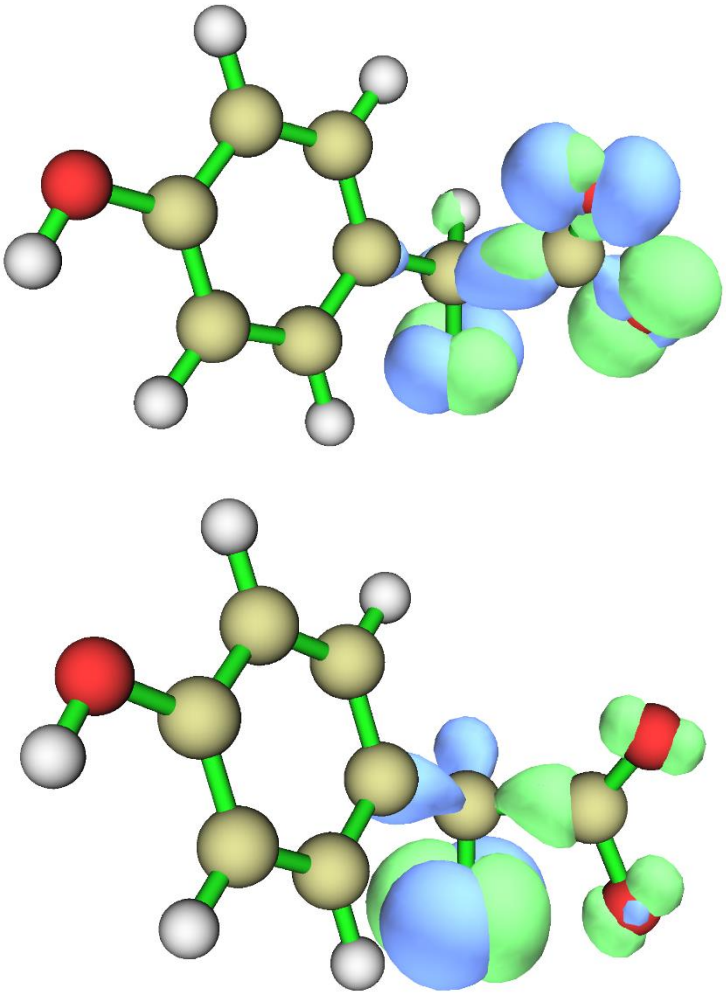

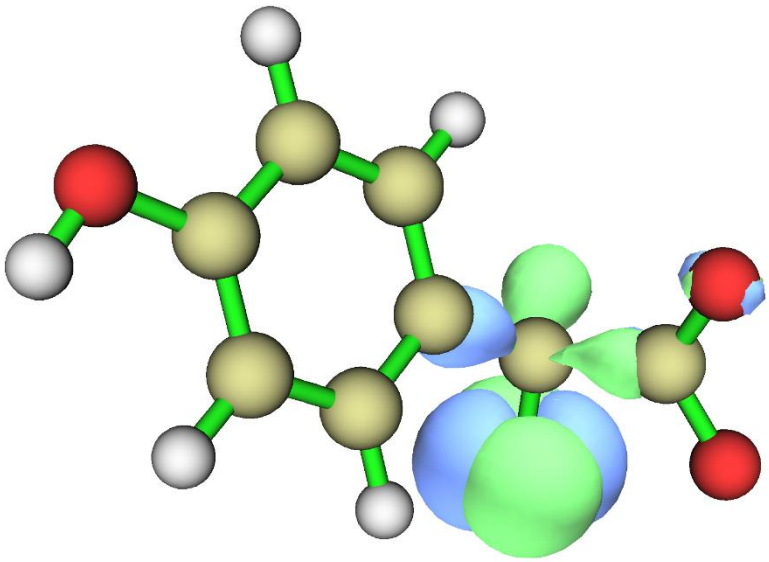

Figure 5 – Simultaneous distribution of hole (in blue) and electron (in green) for $S_0 \rightarrow S_1$ transitions at the following intrinsic reaction coordinates of the thermolysis reaction of Diox-OH: 0.0 (top), 2.3 (middle) and 8.6 (bottom) $amu^{1/2}$ bohr. The distributions were obtained with Multiwfn [46] based on TD ωB97XD/6-31+G(d,p) calculations.

4. Conclusion

Here we have tried to rationalize the role of ET and CT in the singlet intramolecular chemiexcitation step of dioxetanones, a prototypical cyclic peroxide intermediate in CL and BL reactions. To that end, we used a reliable TD-DFT approach to characterize the thermolysis and singlet chemiexcitation step of a model dioxetanone system, at different ionization states.

Our results showed that these dioxetanones undergo thermolysis via a stepwise biradical mechanism, in highly exothermic reactions. However, the ionization state can tune the type of mechanism by which these dioxetanones decompose. Neutral dioxetanones decompose by homolytic cleavage of the peroxide bond, without obvious ET/CT between the dioxetanone ring and the electron-rich moiety, leading to higher ΔE_{act}. By its turn, radical dioxetanones also decompose by homolytic cleavage of the peroxide bond with similar ΔE_{act}, in a reaction with CTIL character. For the contrary, anionic dioxetanones decompose via the CIEEL/CTIL mechanism, with ET-BET/CT-BCT between the peroxide ring and the ionized electron-rich moiety, with significantly lower ΔE_{act}. These results are in agreement with previous theoretical studies of different dioxetanone systems. Finally, our results showed that the ΔE_{act} is determined by the interaction between the ketone and CO_2 reaction fragments, with CIEEL decreasing ΔE_{act} by reducing repulsive interaction between them.

Analysis of the singlet chemiexcitation step showed that non-CIEEL/CTIL-based dioxetanones showed more efficient chemiexcitation profiles than that of CIEEL/CTIL-based cyclic peroxides. These results are in line with previous experimental studies of imidazopyrazinone species,

which findings indicate that higher CL/BL efficiencies are attributed to the thermolysis of neutral dioxetanones. Furthermore, our results showed that the $S_0 \rightarrow S_1$ transitions for all dioxetanones, both CIEEL/CTIL- and non-CIEEL/CTIL-based, are of the LE type (localized on the peroxide ring). There was no relevant CT upon excitation between the peroxide and the electron-rich moieties. Thus, neither CTIL nor CIEEL appear to be involved in the singlet chemiexcitation transitions themselves.

In summary, our results showed that ET/CT (especially ET) is relevant in determining the ΔE_{act} of the thermolysis reaction but are not associated with efficient intramolecular singlet chemiexcitation. Nevertheless, given their role in decreasing ΔE_{act}, these processes could still be operative in CL and BL reactions involving dioxetanone species. Further investigation should also be performed in how these results, focused on intramolecular thermolysis of dioxetanones, could be expanded to intermolecular processes and other types of high-energy peroxide intermediates (such as dioxetanes).

Conflicts of interest

The authors declare that they have no known competing financial interests or personal relationships that could have appeared to influence the work reported in this paper.

Acknowledgments:

The Portuguese "Fundação para a Ciência e Tecnologia" (FCT, Lisbon) is acknowledged for funding of projects PTDC/QUI-QFI/2870/2020, UIDB/00081/2020 (CIQUP) and UIDB/05748/2020 (GreenUPorto). Luís Pinto da Silva acknowledges funding from FCT under the Scientific Employment Stimulus (CEECIND/01425/2017 / 2021.00768.CEECIND).

References

[1] L. Pinto da Silva, J.C.G. Esteves da Silva, Firefly Chemiluminescence and Bioluminescence: Efficient Generation of Excited States, ChemPhyschem 13 (2012) 2257-2262.

[2] M. Vacher, I.F. Galván, B.W. Ding, S. Schramm, R. Berraud-Pache, P. Naumov, N. Ferré, Y.J. Liu, I. Navizet, D. Roca-Sanjuán, W.J. Baader, R. Lindh, Chemi- and Bioluminescence of Cyclic Peroxides, Chem. Rev. 118 (2018) 6927-6974.

[3] F.A. Augusto, G.A. Souza, S.P. Souza Júnior, M. Khalid, W.J. Baader, Efficiency of Electron Transfer Initiated Chemiluminescence, Photochem. Photobiol. 89 (2013), 1299-1317.

[4] T. Mikroulis, M.C. Cuquerella, A. Giussani, A. Pantelia, G.M. Rodríguez-Muniz, G. Rotas, D. Roca-Sanjuán, M.A. Miranda, G.C. Vougioukalakis, Bulding a Functionalizable, Potent Chemiluminescent Agent: A Rational Design Study on 6,8-Substituted Luminol Derivatives, J. Org. Chem. 86 (2021) 11388-11398.

[5] S. Gnain, D. Shabat, Self-Immolative Chemiluminescence Polymers: Innate Assimilation of Chemiexcitation in a Domino-like Depolymerization, J. Am. Chem. Soc. 139 (2017) 10002-10008.
[6] M. Cronin, A.R. Akin, K.P. Francis, M. Tangney, In vivo bioluminescence imaging of intratumoral bacteria, Methods Mol. Biol. 1409 (2016) 69-77.
[7] K.M. Grinstead, L. Rowe, C.M. Ensor, S. Joel, P. Daftarian, E. Dikici, J.M. Zingg, S. Daunert, Red-Shifted Aequorin Variants Incorporating Non-Canonical Amino Acids: Applications in In Vivo Imaging, PLoS One 11 (2016) e0158579.
[8] S.M. Marques, F. Peralta, J.C.G. Esteves da Silva, Optimized chromatographic and bioluminescent methods for inorganic pyrophosphate based on its conversion to ATP by firefly luciferase, Talanta 77 (2009) 1497-1503.
[9] L. Pinto da Silva, A. Nunez-Montenegro, C.M. Magalhães, P.J.O. Ferreira, D. Duarte, P. González-Berdullas, J.E. Rodríguez-Borges, N. Vale, J.C.G. Esteves da Silva, Single-molecule chemiluminescent photosensitizer for a self-activating and tumor-selective photodynamic therapy of cancer, Eur. J. Med. Chem. 183 (2019) 111683.
[10] L. Pinto da Silva, C.M. Magalhães, A. Núnez-Montenegro, P.J.O. Ferreira, D. Duarte, J.E. Rodríguez-Borges, N. Vale, J.C.G. Esteves da Silva, Study of the Combination of Self-Activating Photodynamic Therapy and Chemotherapy for Cancer Treatment, Biomolecules 9 (2019) 384.
[11] C.M. Magalhães, P. González-Berdullas, D. Duarte, A.S. Correia, J.E. Rodríguez-Borges, N. Vale, J.C.G. Esteves da Silva, L. Pinto da Silva, Target-Oriented Synthesis of Marine Coelenterazine Derivatives with Anticancer Activity by Applying the Heavy-Atom Effect, Biomedicines 9 (2021) 1199.
[12] A. Boaro, R.A. Reis, C.S. Silva, D.U. Melo, A.G.G.C. Pinto, F.H. Bartoloni, Evidence for the formation of 1,2-dioxetane as a high-energy intermediate and possible chemiexcitation pathways in the chemiluminescence of lophine peroxides, J. Org. Chem. 86 (2021) 6633-6647.
[13] F.A. Augusto, F.H. Bartoloni, A.P.E. Pagano, W.J. Baader, Mechanistic Stuyf of the Peroxyoxalate System in Completely Aqueous Carbonate Buffer, Photochem. Photobiol. 97 (2021) 309-316.
[14] A. Giussani, P. Farahani, D. Martínez-Nunoz, M. Lundberg, R. Lindh, D. Roca-Sanjuán, Molecular basis of the chemiluminescence mechanism of luminol, Chem. Eur. J 25 (2019) 5202-5213.
[15] S. Schramm, I. Navizet, D.P. Karothy, P. Oesau, V. Bensmann, D. Weiss, R. Beckert, P. Naumov, Mechanistic investigations of the 2-coumaranone chemiluminescence, Phys. Chem. Chem. Phys. 19 (2017) 22852-22859.
[16] J. Czechowaska, A. Kawecka, A. Romanowska, M. Marczak, P. Wityk, K. Krzyminski, B Zadykowicz, Chemiluminogenic acridinium salts: a comparison study. Detection of intermediate entities appearing upon light generation. J. Lumin. 187 (2017) 102-112.

[17] C.X. Liu, Q.B. Liu, K. Dong, S.J. Huang, X.K. Yang, A.M. Ren, C.G. Min, G. Liu, Theoretically obtained insight into the effect of basic amino acids on Cypridina bioluminescence, J. Photochem. Photobiol. A 406 (2021) 113000.

[18] L.F.M.L. Ciscato, F.H. Bartoloni, A.S. Colavite, D. Weiss, R. Beckert, S. Schramm, Evidence supporting a 1,2-dioxetanone as an intermediate in the benzofuran-2(3H)-one chemiluminescence, Photochem. Photobiol. Sci. 13 (2014) 32-37.

[19] Z.M. Kaskova, A.S. Tsarkova, I.V. Yampolsky, 1001 lights: luciferins, luciferases, their mechanisms of action and applications in chemical analysis, biology and medicine, Chem. Soc. Rev. 45 (2016) 6048-6077.

[20] C.G. Min, Q.B. Liu, Y. Leng, C.M. Magalhães, S.J. Huang, C.X. Liu, X.K. Yang, L. Pinto da Silva, Mechanistic insight into the chemiluminescent decomposition of cypridina dioxetanone and the chemiluminescent, fluorescent properties of the light emitter of cypridina bioluminescence, J. Chem. Inf. Model. 59 (2019) 4393-4401.

[21] J.Y. Koo, G.B. Schuster, Chemically initiated electron exchange luminescence. A new chemiluminescent reaction path for organic peroxides, J. Am. Chem. Soc. 99 (1977) 6107-6109.

[22] L.H. Catalani, T. Wilson, Electron transfer and chemiluminescence. Two inefficient systems: 1,4-dimethoxy-9,10-diphenylanthracene peroxide and diphenoyl peroxide, J. Am. Chem. Soc. 111 (1989) 2633-2639.

[23] M.A. Oliveira, F.H. Bartoloni, F.A. Augusto, L.F.M.L. Ciscato, E.L. Bastos, W.J. Baader, Revision of Singlet Quantum Yields in the Catalyzed Decomposition of Cyclic Peroxides, J. Org. Chem. 77 (2012) 10537-10544.

[24] B.W. Ding, Y.J. Liu, Bioluminescence of Firefly Squid via Mechanism of Single Electron-Transfer Oxygenation and Charge-Transfer-Induced Luminescence, J. Am. Chem. Soc. 139 (2017) 1106-1119.

[25] B.W. Ding, P. Naumov, Y.J. Liu, Mechanistic insight into marine bioluminescence: photochemistry of the chemiexcited cypridina (sea firefly) lumophore, J. Chem. Theory Comput. 11 (2015) 591-599.

[26] L. Pinto da Silva, R.F.J. Pereira, C.M. Magalhães, J.C.G. Esteves da Silva, Mechanistic Insight into Cypridina Bioluminescence with a Combined Experimental and Theoretical Chemiluminescent Approach, J. Phys. Chem. B 121 (2017) 7862-7871.

[27] T. Hirano, Y. Takahasi, H. Kondo, S. Maki, S. Kojima, H. Ikeda, H. Niwa, The reaction mechanism for the high quantum yield of Cypridina (Vargula) bioluminescence supported by the chemiluminescence of 6-aryl-2-methylimidazo[1,2-a]pyrazin-3(7H)-ones (Cypridina luciferin analogues), Photochem. Photobiol. Sci. 7 (2008) 197-207.

[28] R. Saito, T. Hirano, S. Maki, H. Niwa, Synthesis and chemiluminescent properties of 6,8-diaryl-2-methylimidazo[1,2-a]pyrazin-3(7H)-ones: Systematic investigation of susbtituent effect at para-position of phenyl group at 8-position, J. Photochem. Photobiol. A 293 (2014) 12-25.

[29] C.G. Min, P.J.O. Ferreira, L. Pinto da Silva, Theoretically obtained insight into the mechanism and dioxetanones species responsible for the singlet chemiexcitation of Coelenterazine, J. Photochem. Photobiol. B 174 (2017) 18-26.
[30] C.M. Magalhães, P. González-Berdullas, J.C.G. Esteves da Silva, L. Pinto da Silva, Elucidating the chemiexcitation of dioxetanones by replacing the peroxide bond with S-S, N-N and C-C bonds, New. J. Chem. 45 (2021) 18518-18527.
[31] C.M. Magalhães, J.C.G. Esteves da Silva, L. Pinto da Silva, Study of coelenterazine luminescence: electrostatic interactions as the controlling factor for efficient chemiexcitation, J. Lumin. 199 (2018) 339-347.
[32] L. Pinto da Silva, C.M. Magalhães, D.M.A. Crista, J.C.G. Esteves da Silva, Theoretical modulation of singlet/triplet chemiexcitation of chemiluminescent imidazopyrazinone dioxetanone via C_8-substitution, Photochem. Photobiol. Sci. 16 (2017) 897-907.
[33] L. Yue, Y.J. Liu, W.H. Fang, Mechanistic insight into the chemiluminescent decomposition of firefly dioxetanone, J. Am. Chem. Soc. 134 (2012) 11632-11639.
[34] M.Y. Wang, Y.J. Liu, Chemistry in Fungal Bioluminescence: A Theoretical Study from Luciferin to light-Emission, J. Org. Chem. 86 (2021) 1874-1881.
[35] M.A. Tzani, D.K. Gioftsidou, M.G. Kallitsakis, N.V. Pliatsios, N.P. Kalogiouri, P.A. Angaridis, I.N. Lykakis, M.A. Terzidis, Direct and indirect chemiluminescence: reactions, mechanisms and challenges, Molecules 26 (2021) 7664.
[36] J.D. Chain, M. Head-Gordon, Long-range corrected hybrid density functionals with damped atom-atom dispersion corrections, Phys. Chem. Chem. Phys. 10 (2008) 6615-6620.
[37] C. Adamo, D. Jacquemin, The calculations of excited-state properties with Time-Dependent Density Functional Theory, Chem. Soc. Rev. 42 (2013) 845-856.
[38] M.J. Frisch, et al., Gaussian 09, Revision D.01, Gaussian, Inc., Wallingford CT, 2013.
[39] D.H. Ess, K.N. Houk, Distortion/Interaction Energy Control of 1,3-Dipolar Cycloaddition Reactivity, J. Am. Chem. Soc. 129 (2007) 10646-10647.
[40] F.M. Bicjelhaupt, K.N. Houk, Analyzing reaction rates with the distortion/interaction-activation strain model, Angew. Chem. Int. Ed. 56 (2017) 10070-10086.
[41] L. Pinto da Silva, C.M. Magalhães, Mechanistic insights into the efficient intramolecular chemiexcitation of dioxetanones from TD-DFT and multireference calculations, Int. J. Quantum Chem. 119 (2019) e25881.
[42] L. De Vico, Y.J. Liu, J.W. Krogh, R. Lindh, Chemiluminescence of 1,2-dioxetane. Reaction Mechanism Uncovered, J. Phys. Chem. A 111 (2007) 8013-8019.
[43] X. Yuan, K. Liu, C. Li, Development of Highly Resioselective Amidyl Radical Cyclization Based on Lone Pair-Lone Pair Repulsion, J. Org. Chem. 73 (2008) 6166-6171.
[44] S.M.G. Sanfeliciano, J.M. Schaus, Rapid assessment of conformation preferences in biaryl and ary carbonyl fragments, PLoS One 13 (2018) e0192974.

[45] A. Fatima, M. Singh, N. Singh, S. Savita, I. Verma, N. Siddiqui, S. Javed, Investigations on experimental, theoretical spectroscopic, electronic excitations, molecular docking of Sulfaguanidide (SG): An antibiotic drug, Chem. Phys. Lett. 783 (2021) 139049.

[46] Y. Takahashi, H. Kondo, S. Maki, H. Niwa, H. Ikeda, T. Hirano, Chemiluminescence of 6-aryl-2-methylimidazo[1,2-a]pyrazin-3(7H)-ones in DMSO/TMG and in diglyme/acetate buffer: support for the chemiexcitation process to generate the singlet-excited state of neutral oxyluciferin in a high quantum yield in the Cypridina (Vargula) bioluminescence mechanism, Tetrahedron Lett. 47 (2006) 6057-6061.

[47] P. Naumov, C. Wu, Y.J. Liu, Y. Ohmiya, Spectrochemistry and artificial color modulation of Cypridina luminescence: indirect evidence for chemiexcitation of a neutral dioxetanone and emission from a neutral amide, Photochem. Photobiol. Sci. 11 (2012) 1151-1155.

[48] L. Pinto da Silva, A.J.M. Santos, J.C.G. Esteves da Silva, Efficient Firefly Chemi/Bioluminescence: Evidence for Chemiexcitation Resulting from the Decomposition of a Neutral Firefly Dioxetanone Molecule, J. Phys. Chem. A 117 (2013) 94-100.

[49] J.J. Snellenburg, S.P. Laptenok, R.J. DeSa, P. Naumov, K.M. Solntsev, Excited-State Dynamics of Oxyluciferin in Firefly Luciferase, J. Am. Chem. Soc. 138 (2016) 16252-16258.

[50] L. Pinto da Silva, R. Simkovitch, D. Huppert, J.C.G. Esteves da Silva, Oxyluciferin Photoacidity: The Missing Element for Solving the Keto-Enol Mystery?, ChemPhysChem 14 (2013) 3441-3446.

[51] L. Yue, Y.J. Liu, W.H. Fang, Mechanistic Insight into the Chemiluminescent Decomposition of Firefly Dioxetanone, J. Am. Chem. Soc. 134 (2012), 11632-11639.

[52] F.H. Bartoloni, M.A. Oliveira, L.F.M.L. Ciscato, F.A. Augusto, E.L. Bastos, W.J. Baader, Chemiluminescence Efficiency of Catalyzed 1,2-Dioxetanone Decomposition Determined by Steric Effects, J. Org. Chem. 80 (2015) 3745-3751.

[53] F.A. Augusto, A. Francés-Monerris, I.F. Galván, D. Roca-Sanjuán, E.L. Bastos, W.J. Baader, R. Lindh, Mechanism of activated chemiluminescence of cyclic peroxides: 1,2-dioxetanes and 1,2-dioxetanones, Phys. Chem. Chem. Phys. 19 (2017) 3955-3962.

[54] T. Lu, F. Chen, Multiwfn: a multifunctinal wavefunction analyzer, J. Comput Chem. 33 (2012) 580-592.

[55] L.F.M.L. Ciscato, F.H. Bartoloni, D. Weiss, R. Beckert, W.J. Baader, Experimental Evidence of the Occurrence of Intramolecular Electron Transfer in Catalyzed 1,2-Dioxetane Decomposition, J. Org. Chem. 75 (2010) 6574-6580.

[56] A.L.P. Nery, D. Weiss, L.H. Catalani, W.J. Baader, Studies on the Intramolecular Electron Transfer Catalyzed Thermolysis of 1,2-Dioxetanes, Tetrahedron 56 (2000) 5317-5327.

[57] A.L.P. Nery, S. Ropke, L.H. Catalani, W.J. Baader. Fluoride-triggered decomposition of m-sililoxyphenyl-substituted dioxetanes by an intramolecular electron transfer (CIEEL) mechanism. Tetrahedron Lett. 40 (1999) 2443-2446.